AFRL-ML-WP-TR-2001-4097

EFFECT OF ALLOYING ADDITIONS ON THE PHASE EQUILIBRIA AND OXIDATION IN THE Mo-Si-B SYSTEM

M.G. MENDIRATTA

UES, Inc.
4401 Dayton-Xenia Road
Dayton, OH 45432-1894

D.M. DIMIDUK

AFRL/MLLM, Building 655
2230 10th Street, Suite 1
Wright-Patterson Air Force Base, OH 45433-7817

APRIL 2001

INTERIM REPORT FOR PERIOD 30 JUNE 1998 – 30 JUNE 2000

MATERIALS AND MANUFACTURING DIRECTORATE
AIR FORCE RESEARCH LABORATORY
AIR FORCE MATERIEL COMMAND
WRIGHT-PATTERSON AIR FORCE BASE, OH 45433-7750

NOTICE

WHEN GOVERNMENT DRAWINGS, SPECIFICATIONS, OR OTHER DATA ARE USED FOR ANY PURPOSE OTHER THAN IN CONNECTION WITH A DEFINITELY GOVERNMENT-RELATED PROCUREMENT, THE UNITED STATES GOVERNMENT INCURS NO RESPONSIBILITY OR ANY OBLIGATION WHATSOEVER. THE FACT THAT THE GOVERNMENT MAY HAVE FORMULATED OR IN ANY WAY SUPPLIED THE SAID DRAWINGS, SPECIFICATIONS, OR OTHER DATA, IS NOT TO BE REGARDED BY IMPLICATION OR OTHERWISE IN ANY MANNER CONSTRUED, AS LICENSING THE HOLDER OR ANY OTHER PERSON OR CORPORATION, OR AS CONVEYING ANY RIGHTS OR PERMISSION TO MANUFACTURE, USE, OR SELL ANY PATENTED INVENTION THAT MAY IN ANY WAY BE RELATED THERETO.

THIS REPORT IS RELEASABLE TO THE NATIONAL TECHNICAL INFORMATION SERVICE (NTIS). AT NTIS, IT WILL BE AVAILABLE TO THE GENERAL PUBLIC, INCLUDING FOREIGN NATIONS.

THIS TECHNICAL REPORT HAS BEEN REVIEWED AND IS APPROVED FOR PUBLICATION.

G. Brandt Miller

GERALD B. MILLER, Captain
Project Engineer
Metals Branch
Metals, Ceramics & NDE Division
Materials & Manufacturing Directorate

Katherine A. Stevens

KATHERINE A. STEVENS, Chief
Metals Branch
Metals, Ceramics & NDE Division
Materials & Manufacturing Directorate

Gerald J. Petrak

GERALD J. PETRAK, Assistant Chief
Metals, Ceramics & NDE Division
Materials & Manufacturing Directorate

IF YOUR ADDRESS HAS CHANGED, IF YOU WISH TO BE REMOVED FROM OUR MAILING LIST, OR IF THE ADDRESSEE IS NO LONGER EMPLOYED BY YOUR ORGANIZATION, PLEASE NOTIFY, AFRL/MLLM, WRIGHT-PATTERSON AFB, OH 45433-7817 TO HELP US MAINTAIN A CURRENT MAILING LIST.

COPIES OF THIS REPORT SHOULD NOT BE RETURNED UNLESS RETURN IS REQUIRED BY SECURITY CONSIDERATIONS, CONTRACTUAL OBLIGATIONS, OR NOTICE ON A SPECIFIC DOCUMENT.

REPORT DOCUMENTATION PAGE	Form Approved OMB No. 0704-0188

1. AGENCY USE ONLY *(Leave blank)*	2. REPORT DATE	3. REPORT TYPE AND DATES COVERED
	April 2001	INTERIM REPORT: 6/30/1998 - 6/30/2000

4. TITLE AND SUBTITLE
Effect of Alloying Additions on the Phase Equilibria and Oxidation in the Mo-Si-B System

5. FUNDING NUMBERS
C: F33615-96-C-5258
PE: 62102F
PR: 2306
TA: B0
WV: 02

6. AUTHOR(S)
M.G. Mendiratta, UES, Inc.
D.M. Dimiduk, AFRL/MLLM

7. PERFORMING ORGANIZATION NAME(S) AND ADDRESS(ES)

UES, Inc.	D.M. Dimiduk
4401 Dayton-Xenia Road	10th Street, Suite 1
Dayton, OH 45432-1894	Wright-Patterson AFB, OH 45433-7817

8. PERFORMING ORGANIZATION REPORT NUMBER

9. SPONSORING/MONITORING AGENCY NAME(S) AND ADDRESS(ES)
Materials and Manufacturing Directorate
Air Force ResearchLaboratory
Air Force Materiel Command
Wright-Patterson AFB, OH 45433-7750
POC: D.M. Dimiduk, AFRL/MLLM, 937-255-9839

10. SPONSORING/MONITORING AGENCY REPORT NUMBER
AFRL-ML-WP-TR-2001-4097

11. SUPPLEMENTARY NOTES

12a. DISTRIBUTION AVAILABILITY STATEMENT
Approved for public release; distribution is unlimited.

12b. DISTRIBUTION CODE

13. ABSTRACT *(Maximum 200 words)*
The Mo-Si-B alloys containing the Mo metal phase in equilibrium with the Mo3Si and Mo5SiB2 intermetallic phases have potential as hot-section materials for jet engines. For high-pressure turbine blade application, the ternary Mo-Si-B compositions exhibit adequate oxidation resistance in the temperature range of 1000 to 1300 °C, but below 1000 °C, the oxidation resistance is not good. The present study was undertaken to explore the effect of a number of alloying additions to a ternary Mo-Si-B Base on improving the oxidation resistance. Microstructures and phase equilibria were determined at selected temperatures of quaternary and quinary alloys. The elements added were W, Nb, V, Cr, Re, Ge, A1, Hf and Ti+Cr. These alloys did not produce a better oxidation resistance-composition than the base ternary Mo-Si-B alloy.

14. SUBJECT TERMS	15. NUMBER OF PAGES
Mo-Si-B Alloys, Microstructures, Phase Equilibria, Oxidation Resistance	50
	16. PRICE CODE

17. SECURITY CLASSIFICATION OF REPORT	18. SECURITY CLASSIFICATION OF THIS PAGE	19. SECURITY CLASSIFICATION OF ABSTRACT	20. LIMITATION OF ABSTRACT
UNLCASSIFIED	UNCLASSIFIED	UNCLASSIFIED	SAR

TABLE OF CONTENTS

LIST OF FIGURES

Figure **Page**

LIST OF FIGURES (Concluded)

LIST OF TABLES

FOREWORD

The work presented in this report was supported in part by Air Force Contract F33615-96-C-5258, and Captain Gerald B. Miller of the Materials Development Branch, AFRL/MLL, was the Government Project Engineer. The research reported herein covered the period of 30 June 1998 to 30 June 2000.

1. Introduction

Mo-based alloys possess excellent high-temperature mechanical properties. However, their widespread use for structural applications involving long service at high temperatures has been hampered by their very poor oxidation resistance. Limited improvements in oxidation protection have been demonstrated with alloying and coatings [1-3], but the possibility of catastrophic failure from oxidation still exists. Recently it has been shown [4-5] that there is a possibility for enhanced oxidation resistance of Mo in equilibrium with Mo_3Si and Mo_5SiB_2 phases in the Mo-Si-B system. Investigation of mechanisms governing the oxidation behavior have been carried out on composition within this ternary phase field for temperatures ranging from 600 to 1400 °C [6-7]. In addition, some studies have also been conducted on microstructural evaluation and phase relations [8-9] and mechanical properties [10-12].

The present investigation was undertaken to determine the effect of a number of alloying additions to the Mo-Si-B system on 1) modifications in phase equilibrium and microstructures, and 2) possible improvement in the oxidation resistance. The alloying additions are listed in Table 1. The choices of alloying additions are not based upon any known effects and are mostly empirical.

Table 1. Compositions of Quaternary Mo-Si-B-X and Quinary Mo-Si-B-X-Y Alloys

Element	Composition/Composition Range (Atomic Percent)
W	Mo-7.5 to 30W - 15 to 19.5Si - 5 to 10B
Nb	Mo-30Nb-30Si-10B
V	Mo-20 to 30V - 12 to 30Si - 6 to 10B
Cr	Mo-20Cr-12Si-10B
Re	Mo-7.5 to 23Re - 7.5 to 20 Si-10B
Ge	Mo-5Ge-11Si-8B
Al	Mo-5Al-11Si-11B
Hf	Mo-0.3 to 10Hf - 9 to 12Si - 9 to 12B
Ti+Cr	Mo-18Ti-11Cr-9Si-9B

However, the alloying selection was somewhat guided by the published ternary Mo-Si-W [13], Mo-Si-Nb [14], Mo-Si-Cr [15], Mo-Si-V [16], and binary Mo-Re, Re-Si, Mo-Al, Mo-Si, Mo-Hf, Hf-Si, Mo-Ti, and Ti-Si phase diagrams [17]. Mo-Si-W and Mo-Si-Nb phase diagrams exhibit equilibrium between Mo-W solid solution and $(MoW)_5Si_3$ and Mo-Nb solid solution and $(MoNb)_5Si_3$, respectively. Therefore, in the Mo-M-Si-B quaternary (M = W, Nb, respectively) system, a three-phase equilibrium consisting of αMo-$(MoM)_5Si_3$-$(MoM)_5SiB_2$ (T2) phases

is likely to exist. However, the Mo-Si-Cr and Mo-V-Si phase diagrams do not exhibit equilibrium between Mo-M solid solution (M = Cr, V, respectively) and $(MoM)_5Si_3$; rather they show a two-phase equilibria between metal phase + $(MoM)_3Si$ and between $(MoM)_5Si_3$ and $(MoM)_3Si$. Therefore, in the case of Cr and V, it is unlikely that B additions could accomplish the desired three phase αMo-$(MoM)_5Si_3$-T2 equilibrium. Cr was added to find out whether a protective Cr_2O_3-type oxide will form in the intermediate temperature range, i.e., from 650 to 900 °C. V forms V_2O_3, which volatilizes at an even lower temperature than MoO_3; therefore, V was added to determine whether protective B-SiO_2 can form to lower temperatures by volatilization of V and selective oxidation of Si and B. Re was added because Re is known to ductilize Mo and to explore its (unknown) effect on oxidation. Ge was added to modify glass viscosity and thermal expansion coefficient of SiO_2. Al was added to determine its effect on microstructure and oxidation. The last two categories of compositions consisting of Hf and combined Ti + Cr additions are derived from the work by Berczik from Pratt & Whitney to potentially enhance oxidation resistance of their base Mo-Si-B composition [18].

2. Experimental Procedure

The alloys were made as 200-gm cast buttons by nonconsumable triple arc melting of elemental mixtures. The samples machined from these buttons were heat treated in an inert argon atmosphere at temperatures from 1500 to 1700 °C, depending on the elements added. The heat treatment information is given for each composition in the results section. The microstructures were characterized by SEM, X-ray diffraction (XRD), and electron probe microanalysis (EPMA). The samples were chemically analyzed and their compositions were found to be very close to their nominal compositions. The alloys were screened for their oxidation resistance. The cyclic oxidation tests were carried out at two temperatures in static air: 800 °C and 1300 °C. The oxidation cyclic consisted of an initial exposure of half an hour at temperature, withdrawing the sample from the furnace and cooling it to room temperature, weighing the sample, and putting it back in the furnace. The cyclic time interval was gradually increased after a first few cycles. The selection of exposure temperatures is based upon a previous study [6] which indicated that these two temperatures correspond to important aspects of the overall behavior. The kinetic weight change data and the macro/micro observations of oxide scales and changes in sample shape and integrity exhibited the degree of oxidation resistance. The oxidation behavior of the present composition was compared to that for the ternary Mo-11Si-11B (all compositions in at.%), which will be published elsewhere [6].

3. Results

3.1 Mo-Si-W-B Alloys

3.1.1 Phase Relations

Table 2 gives compositions of all of the alloys explored and the phases as determined by EPMA and XRD in the present study. Table 3 provides the chemical makeup of the selected alloys as revealed by EPMA. The first three alloys in Table 2 are the ternary alloys without boron and were selected to confirm the published phase relations [13]. These show, starting from the Mo corner, three-phase fields with increasing W and Si contents. These are as follows: 1) Mo(W) metal + $(MoW)_3Si$, 2) Mo(W) metal + $(MoW)_3Si$ + $(MoW)_5Si_3$, and 3) Mo(W) + $(MoW)_5Si_3$. Therefore, in the ternary alloy system, it is possible to obtain the metal phase + 5:3 silicide equilibrium, e.g., at 10 at.% Si, a W level of $\geq$ 30 at.% is needed to get to this two-phase field. The present work (Tables 2 & 3) essentially confirmed the published phase relations.

Table 2. Nominal Compositions (Atomic Percent) of Mo-W-Si-B Alloys and Phases Found

Composition	Phases
1. Mo-15W-5Si	αMo(W) + $(MoW)_3Si$
2. Mo-30W-5Si	αMo(W) + $(MoW)_3Si$ + $(MoW)_5Si_3$
3. Mo-20W-20Si	αMo(W) +$(MoW)_3Si$ + $(MoW)_5Si_3$
4. Mo-19.5W-19.5Si-2.5B	αMo(W) + $(MoW)_5Si_3$ + T2
5. Mo-18.5W-18.5Si-7.5B	αMo(W) + $(MoW)_5Si_3$ + T2
6. Mo-18W-17Si-10B	αMo(W) + $(MoW)_5Si_3$ + T2
7. Mo-30W-19Si-10B	αMo(W) + $(MoW)_5Si_3$ + T2
8. Mo-7.5W-18Si-10B	αMo(W) + $(MoW)_3Si$ + T2
9. Mo-8W-15Si-10B	αMo(W) + $(MoW)_3Si$ + T2

Heat Treatment: 1600 °C/24 hr +1700 °C/48 hr

Table 3. Chemistry of the Phases as Determined by EPMA in the Selected Mo-W-Si-B Alloys

Alloy: Mo-18W-17Si-10B			
Element	**Metal Phase**	**$(MoW)_5Si_3$**	**$(MoW)_5SiB_2$(T2)**
Mo	50.3	56.3	48.1
W	29.7	5.8	15.3
Si	2.6	37.9	12.4
B	17.4	-	24.2

Alloy: Mo-30W-19Si-10B		
Element	**Metal Phase**	**$(MoW)_5Si_3$**
MO	30.2	48.8
W	56.4	13.6
SI	1.1	37.6
B	12.3	-

Alloy: Mo-7.5W-18Si-10B			
Element	**Metal Phase**	**$(MoW)_3Si$**	**$(MoW)_5SiB_2$ (T2)**
Mo	66.3	70.4	52.9
W	22.3	4.8	6.7
Si	2.7	24.8	12.1
B	8.7	-	28.3

Alloy: Mo-8W-15Si-10B			
Element	**Metal Phase**	**$(MoW)_3Si$**	**$(MoW)_5SiB_2$ (T2)**
Mo	72.1	71.5	50.5
W	16.5	3.7	5.5
Si	2.8	24.8	11.4
B	8.6	-	32.6

In the quaternary Mo-W-Si-B alloys, in addition to the phase described above, the T2 phase was found to be present.

Figure 1 schematically depicts the Mo-rich corner of the four-component phase equilibria at 1700 °C.

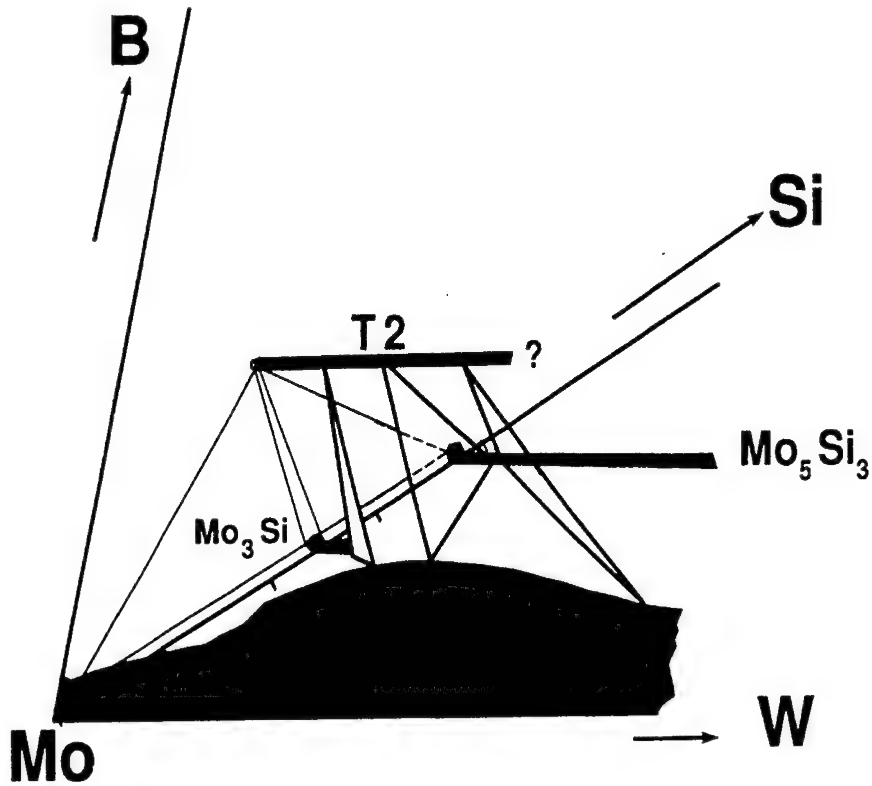

Figure 1. Schematic Representation of Quaternary Mo-W-Si-B Phase Diagram 1700 °C Isotherm

Thus, it was possible to obtain the metal + 5:3 silicide + T2 three-phase field. It was estimated that for 10 at.% Si and 10 at.% B, a minimum of ~ 25 at.% W was required to get to this three-phase field.

3.1.2 Oxidation Behavior

For the ternary Mo-Si-B compositions under cyclic oxidation exposures at both 800 °C and 1300 °C, the shape and physical appearance of the samples remained intact for a large number of cycles for total times of up to 200 hours [6]. However, for many quaternary alloys the shape became highly distorted with swelling, exfoilation and delamination after only a few cycles and, based on physical appearance, the tests were stopped. Therefore, the weight change data are limited, and in some cases, show only the initial trend.

Figures 2 and 3 show the kinetic data at 800 °C and 1300 °C for selected Mo-W-Si-B alloys.

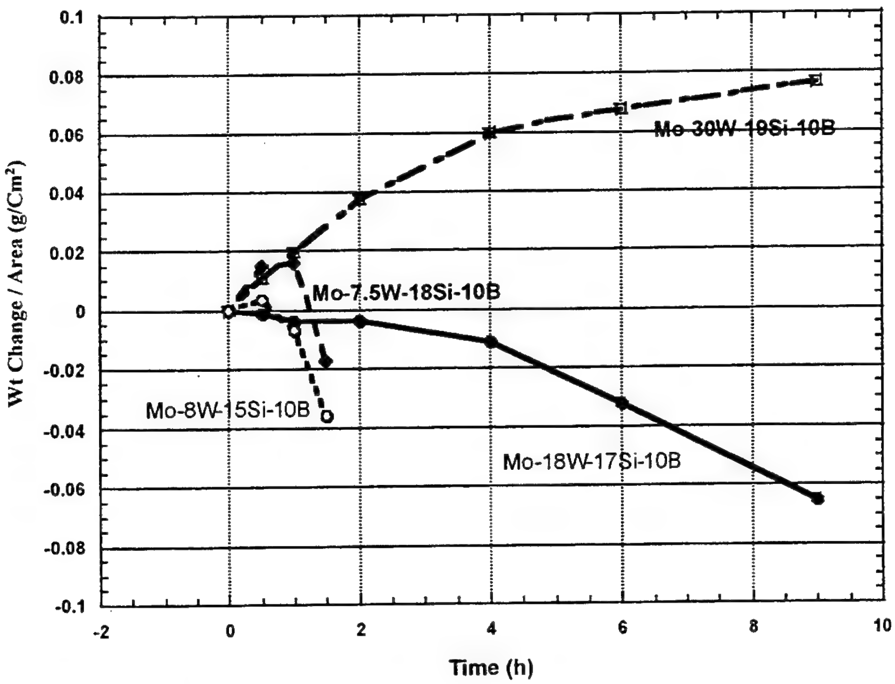

Figure 2. Cyclic Oxidation Kenetics for Selected Mo-Si-B-W Alloys: 800 °C

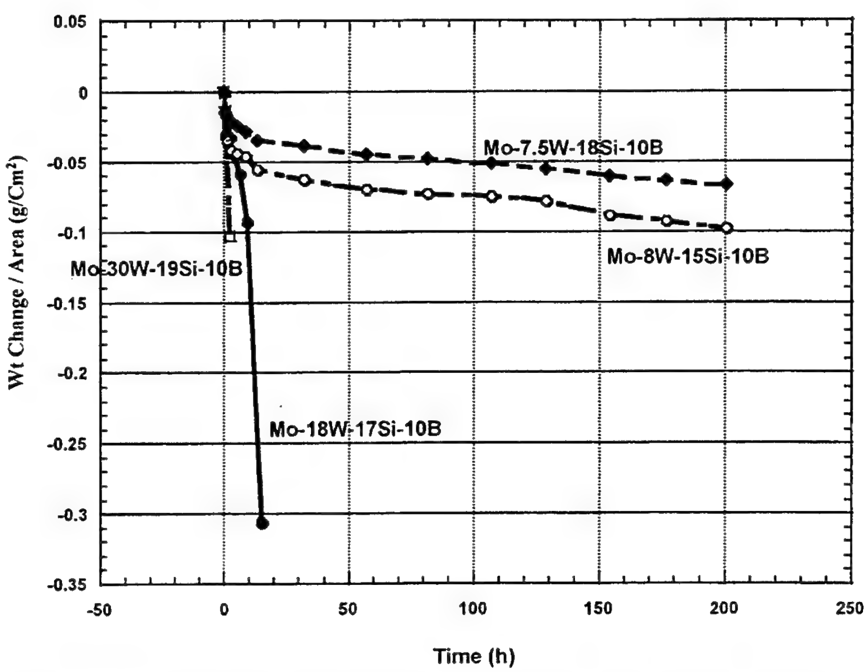

Figure 3. Cyclic Oxidation Kenetics for Selected Mo-Si-B-W Alloys: 1300 °C

At 800 °C, in one case there was considerable weight gain (as opposed to weight loss); however, in all cases there was severe physical distortion of the samples after only a few cycles, indicating imminent disintegration, and the tests were stopped.

Figure 4 displays the macro photos of the samples after exposure at 800 °C (caption shows the compositions) that exhibited considerable swelling and severe delamination.

Mo-18W-17Si-10B
800°C / 9h

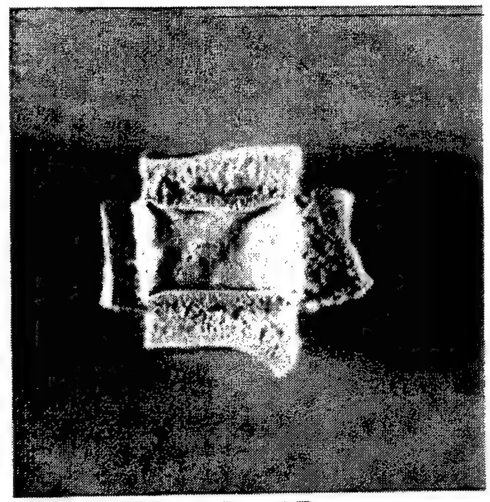

Mo-30W-19Si-10B
800°C / 9h

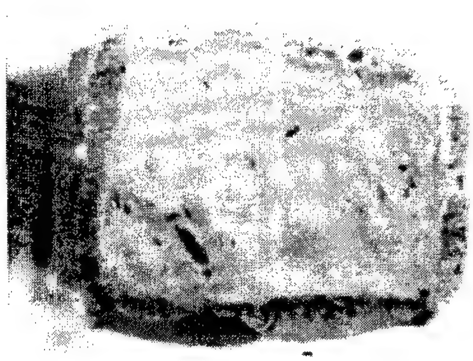

Mo-7.5W-18Si-10B
800°C / 1.5h

Mo-8W-15Si-10B
800°C / 1.5h

Figure 4. Swelling, Exfoliation and Delamination of Selected Mo-W-Si-B Alloys Exposed at 800 °C

Thus, the 800 °C oxidation resistance of the W-containing alloys was much inferior to that for the Mo-11Si-11B alloy [6]. At 1300° C, the kinetic data exhibit very high weight losses for high-W-containing alloys (Mo-30W-19Si-10B and Mo-18W-17Si-10B) in the first few cycles. For the low W containing alloys (Mo-7.5W-18Si-10B and Mo-8W-15Si-10B), the behavior was somewhat similar to the ternary Mo-11Si-11B alloy although with slightly greater weight loss. The physical shape of the W-containing alloys exposed at 1300 °C remained relatively intact.

3.2 Mo-Nb-Si-B, Mo-Cr-Si-B Alloys

3.2.1 Phase Relations:

Only one composition each for Nb and Cr was explored. Table 4 shows the chemistry of phases determined by EPMA.

Table 4. Phase Chemistry Determined by EPMA for Mo-Nb-Si-B and Mo-Cr-Si-B Alloys

Alloy: Mo-30Nb-30Si-10B			
Element	**T2**	**$(MoNb)_5Si_3$**	**$(NbMo)_5Si_3$**
Mo	33.5	34.4	22.2
Nb	29.5	27.8	39.1
Si	14.9	37.8	37.5
B	22.1	-	1.2

Alloy: Mo-20Cr-12Si-10B				
Element	**Metal Phase**	**$(MoCr)_3Si$**	**T2(1)**	**T2(2)**
Mo	74.4	53.3	52.8	46.8
Cr	23.1	24.1	11.4	17.3
Si	1.7	22.6	10.7	11.8
B	0.8	-	25.1	24.1

Alloys Heat Treatment: 1500 °C/100 hr + 1400 °C/100 hr.

In the Nb-containing alloy, as given in Table 4, the phases present were T2 phase and two 5:3 silicides (one Mo-rich and the other Nb-rich). The published Mo-Nb-Si ternary-phase diagram reveals the existence of a two-phase metal + 5:3 silicide field for Nb $\geq$ 29 at.%, and Si contents ranging from 5 to 30 at.%. In the quaternary Mo-Nb-Si-B system, it is very likely that a three-phase field consisting of metal phase (i.e., solid solution of Nb in Mo) + 5:3 silicide + T2 exists for a Si content slightly less than the present alloy. The

ternary Mo-Nb-Si phase diagram also shows a Mo(Nb) + $(MoNb)_3Si$ two phase field for Nb $\leq$ 25 at.% and Si between 2.5 to ~ 23 at.%. Addition of B in this composition range is likely to produce a metal + T2 + 3:1 silicide equilibrium. A possible schematic construct of the Mo-rich corner of the Mo-Nb-Si-B phase diagram is given in Figure 5.

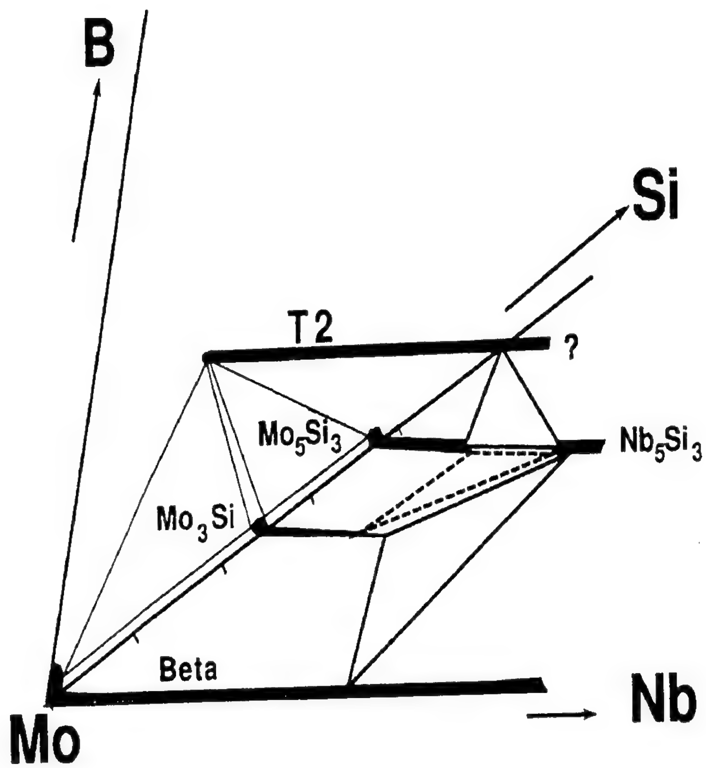

Figure 5. Possible Phase Diagram at 1400 °C for Mo-Rich Corner of the Mo-Nb-Si-B System

For the Cr-containing alloy, the phases found were metal phase + $(MoCr)_3Si$ and two T2-type phases with different Mo and Cr levels. The published Mo-Cr-Si phase diagram exhibits continuous Mo-Cr solid solution in equilibrium with a continuous solid solution of Mo_3Si and Cr_3Si and also a two-phase field between $(MoCr)_3Si$ and $(MoCr)_5Si_3$. Thus, it was highly unlikely that addition of B would produce an equilibrium between the metal phase, the 5:3 silicide, and the T2 phase.

Our experiments suggest that the Mo-Cr-Si-B phase diagram may be like that shown schematically in Figure 6.

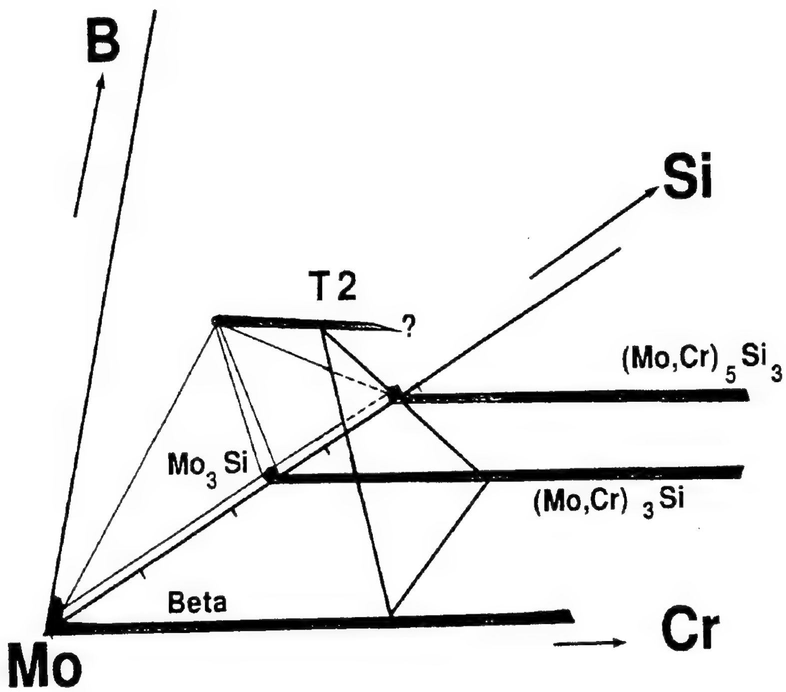

Figure 6. Schematic Phase Diagram Construct at 1400 °C for the Mo-Rich Corner of the Mo-Cr-Si-B System

3.2.2 Oxidation Behavior

For the Nb-containing alloy, even though there was no metal phase present, cyclic oxidation exposure was performed to examine the oxidation resistance for a combination of Nb-containing T2 and 5:3 silicide phases. If the resistance is not good then, most probably, Nb is not a viable alloying addition because, for a modified composition which produces metal phase in equilibrium with the T2 and 5:3 silicide, the oxidation rate is expected to be worse.

Figures 7 and 8 show the weight change data for the Nb-and Cr-containing alloys at 800°C and 1300°C, respectively.

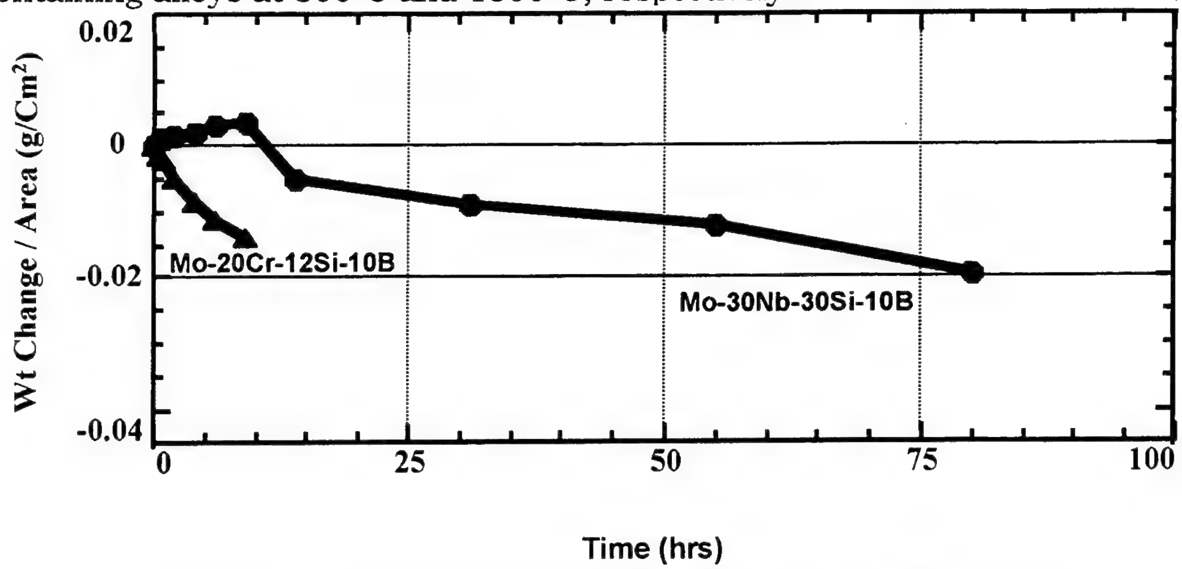

Figure 7. Cyclic Oxidation Kinetics for the Nb- and Cr-Containing Mo-Si-B Alloys: 800 °C

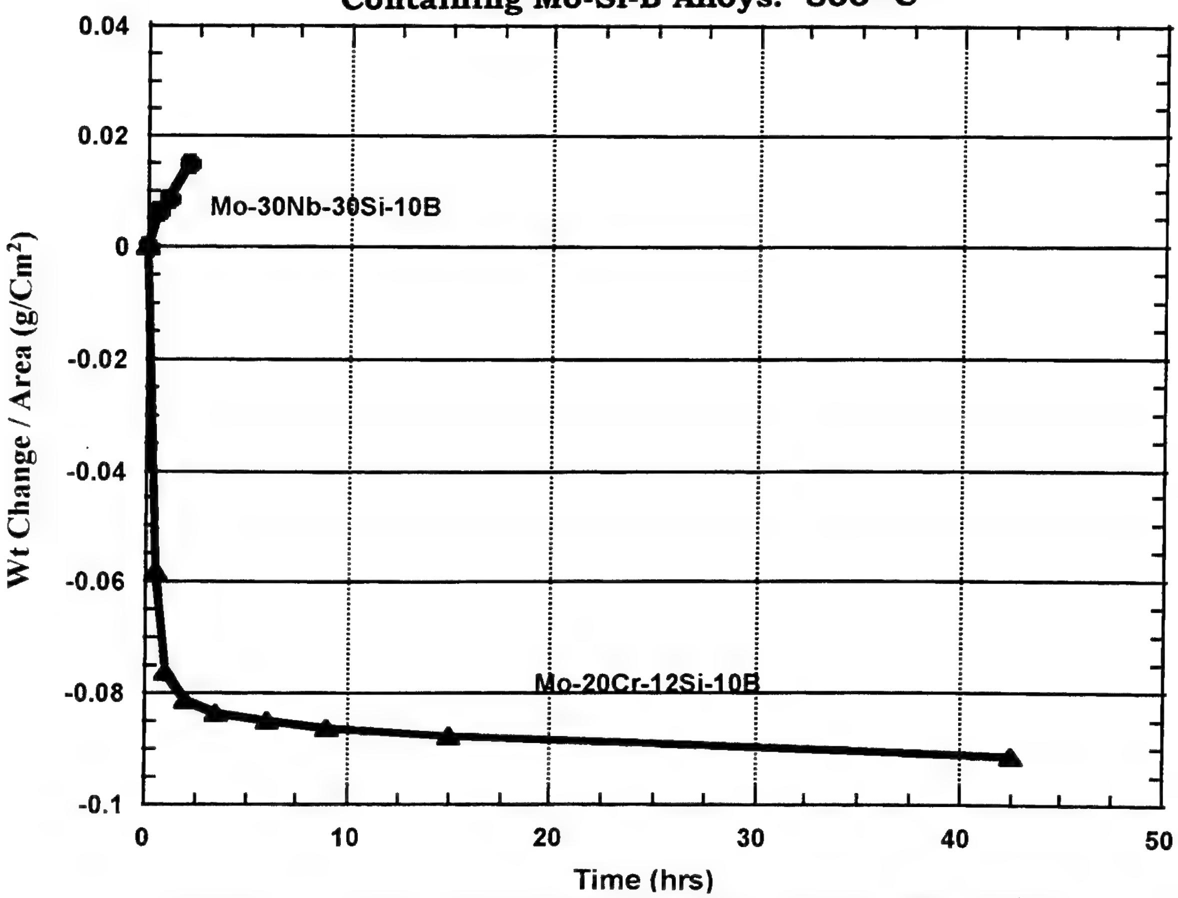

Figure 8. Cyclic Oxidation Kinetics for the Nb- and Cr-Containing Mo-Si-B Alloys: 1300 °C

Figure 9 contains the macro photographs of these alloys after different oxidation exposures.

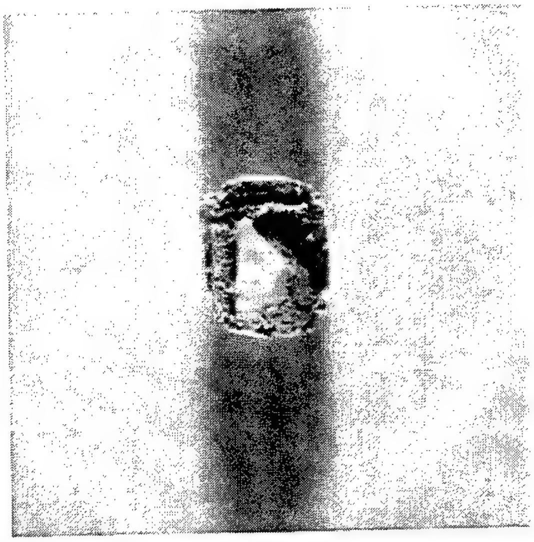

Mo-30Nb-30Si-10B
800^{0}C / 80h

Mo-20Cr-12Si-10B
800^{0}C / 9h

Mo-30Cr-30Si-10B
1300^{0}C / 2h

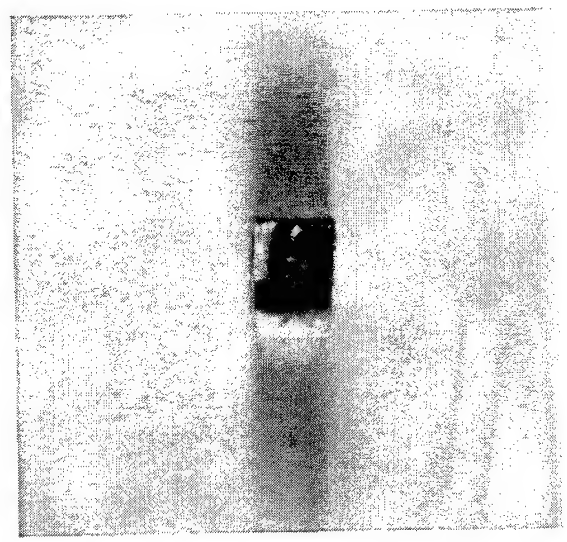

Mo-20Cr-12Si-10B
1300^{0}C / 43h

Figure 9. Macro Photographs Exhibiting Sample Shape Change (Swelling, Delamination) for Nb- and Cr-Containing Mo-Si-B Alloys for 800 ° C and 1300 °C Oxidation Exposure

Even though at 800 °C there is very small weight loss for the Nb-containing alloy up to 80 hours, the macro picture clearly exhibits flaking and imminent delamination. For the Cr-containing alloy, massive delamination had already happened by nine hours at 800 °C. At 1300 °C, the Nb-containing alloy gained weight for 2 hours; however, as shown by the macro picture, the sample exhibited significant distortion due to nonuniform swelling. The Cr-containing alloy at 1300 °C lost significantly more weight than the Mo-11Si-11B, and therefore, even though the sample shape was intact, the test was stopped after 43 hours.

3.3. Mo-V-Si-B Alloys

3.3.1 Phase Relations

The ternary Mo-V-Si phase diagram from the literature [16] shows two, two-phase fields with increasing Si. These are αMoV (metal phase) + $(MoV)_3Si$, and $(MoV)_3Si$ + $(MoV)_5Si_3$. The B additions in the present alloys simply produces an additional T2 phase, resulting in metal phase + 3:1 silicide + T2, and 3:1 silicide + 5:3 silicide + T2 phase fields. The EPMA chemistry data for various phases are given in Table 5 for selected V-containing alloys.

Table 5. Phase Chemistry Determined by EPMA for Selected Mo-V-Si-B Alloys.

Alloy: Mo-30V-30Si-10B				
Element	**$(MoV)_5Si_3$**	**$(VMo)_5Si_3$**	**T2**	**(VMo)B**
Mo	32.5	28.3	33.2	18.8
V	29.6	33.6	31.3	34.4
Si	37.9	38.1	13.2	0.12
B	-		22.3	46.7

Alloy: Mo-20V-22Si-8B		
Element	**$(MoV)_3Si$**	**T2**
Mo	54.1	44.5
V	21.5	22.1
Si	-	12.9
B	-	20.5

Alloy: Mo-30V-22Si-8B			
Element	**$(MoV)_3Si$**	**$(MoV)_5Si_3$**	**T2**
Mo	42.5	35.1	36.8
V	32.4	28.2	27.8
Si	25.1	36.7	12.7
B	-	-	22.7

Alloy: Mo-30V-15Si-8B			
Element	**Metal Phase**	**$(MoV)_3Si$**	**T2**
Mo	66.2	44.1	36.1
V	31.5	32.7	28.3
Si	2.3	23.2	11.5
B	-		24.1

Heat Treatment: 1600 °C/24 hr +1700 °C/48 hr

From the phases present for the ternary and quaternary compositions, it is clear that a metal phase + 5:3 silicide + T2 equilibrium is not possible in this system. A possible quaternary phase diagram representation is given by Figure 10.

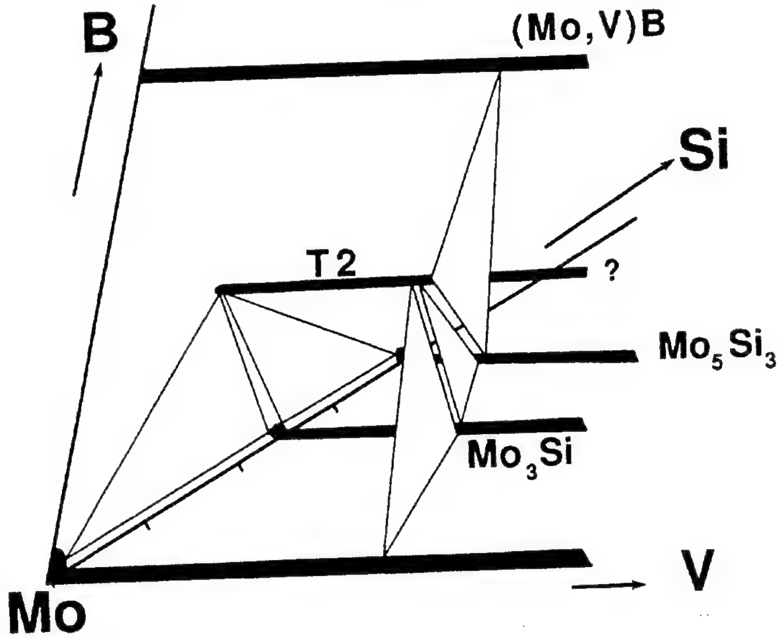

Figure 10. Schematic 1700 °C Isotherm Construct for the Mo-Rich Corner of the Mo-V-Si-B System

3.3.2 Oxidation Behavior

The weight change data for the Mo-30V-30Si-10B [$(MoV)_5Si_3$ + $(VMo)_5Si_3$ + T2 + (VMo)B)] alloy at 800 °C and 1300 °C are shown in Figure 11.

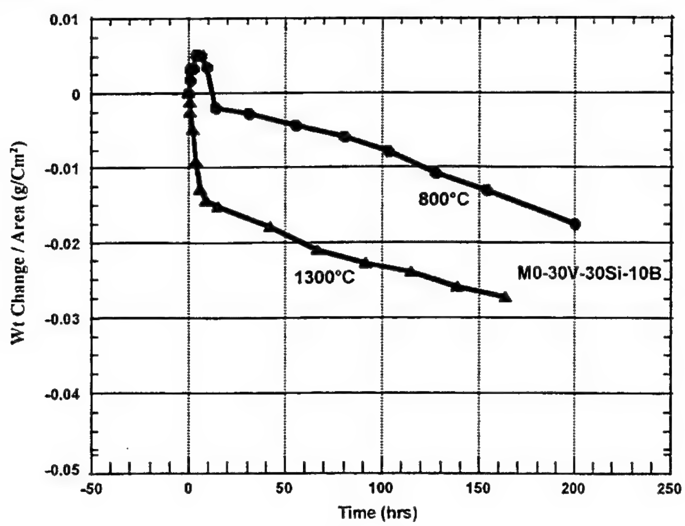

Figure 11. Cyclic Oxidation Kinetics for the Mo-30V-30Si-10B at 800 °C and 1300 °C

The weight loss per unit area is small at both temperatures and compared favorably with the base Mo-11Si-11B. Also, the physical shape of the samples was intact after the cyclic oxidation exposures. Thus in this composition, the oxidation protection is good. However, this alloy contains high levels of Si and there is no metal phase present. When the Si level was decreased, the oxidation resistance significantly decreased. Figures 12 and 13 are the oxidation kinetic data at 800 °C and 1300 °C for the compositions investigated.

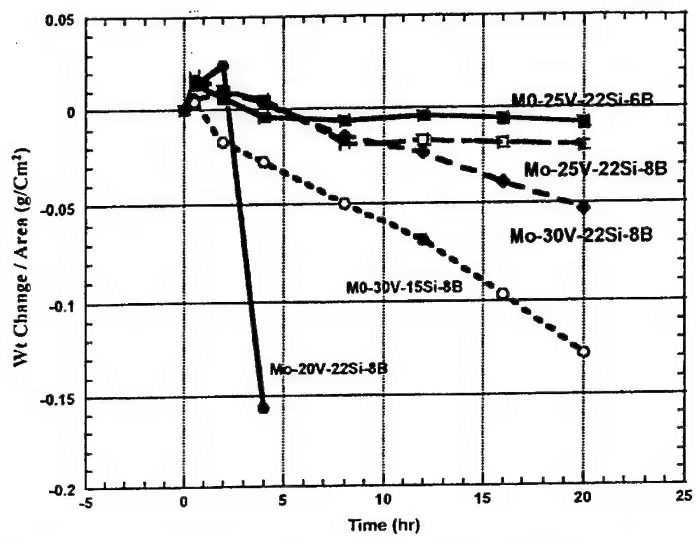

Figure 12. Cyclic Oxidation Kinetics for the Selected V-Containing Mo-Si-B Alloys for 800 °C

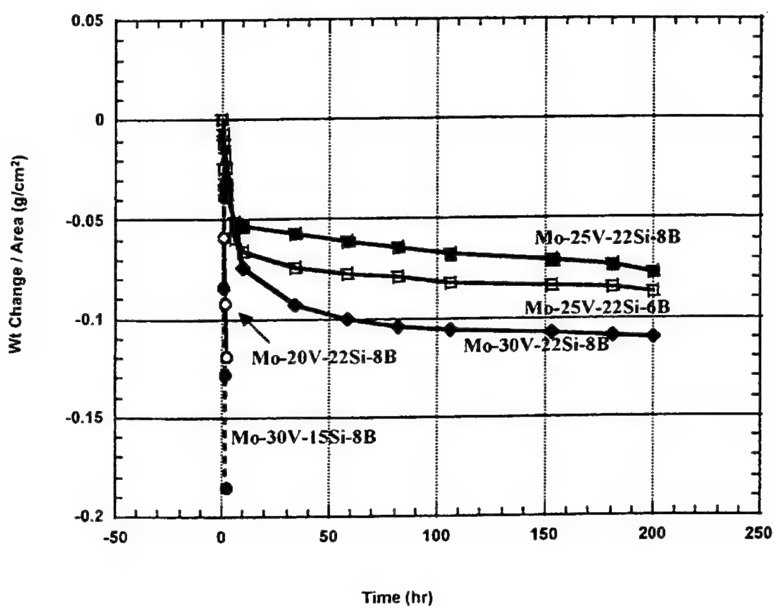

Figure 13. Cyclic Oxidation Kinetics for the Selected V-Containing Mo-Si-B Alloys for 1300 °C

The compositions are given on each curve. At 800 °C, a number of compositions exhibited comparable weight losses to the base Mo-11Si-11B; however, as shown in Figure 14, physically the oxide products did not appear protective at all, indicating delamination, swelling, shape distortion & porosity.

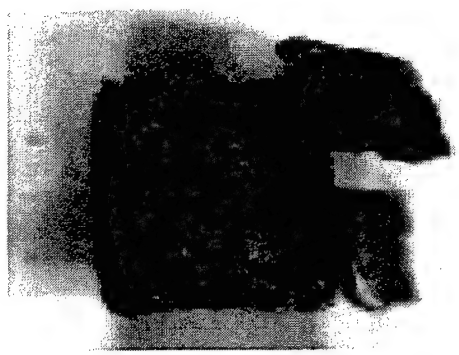

Mo-20V-22Si-8B
800°C / 4h

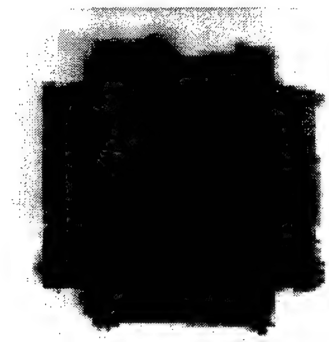

Mo-25V-22Si-8B
800°C / 20h

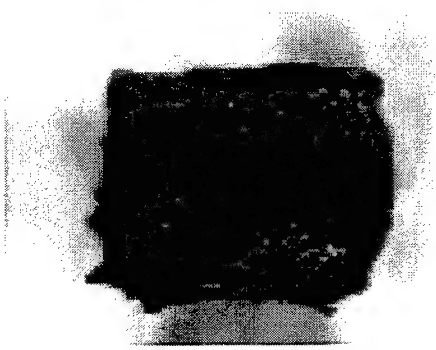

Mo-30V-22Si-8B
800°C / 20h

Mo-30V-15Si-8B
800°C / 20h

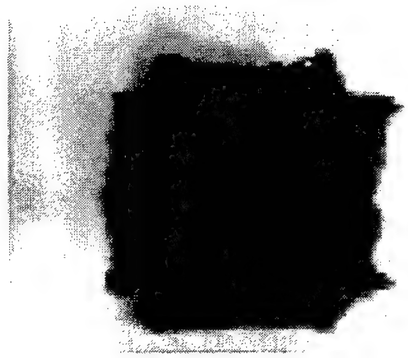

Mo-25V-22Si-6B
800°C / 20h

Figure 14. Macrophotographs of Selected Mo-Si-B-V Alloys Exhibiting Swelling and Delamination at 800°C

At 1300 °C, as shown in Figure 13, the selected compositions exhibited weight losses significantly higher than Mo-11Si-11b. The shapes of the 1300 °C exposed samples are shown in Figure 15.

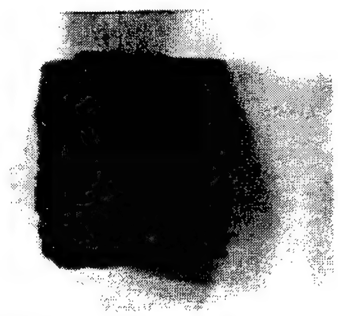

Mo-20V-22Si-8B
1300°C / 2h

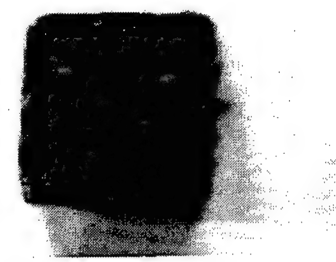

Mo-25V-22Si-8B
1300°C / 200h

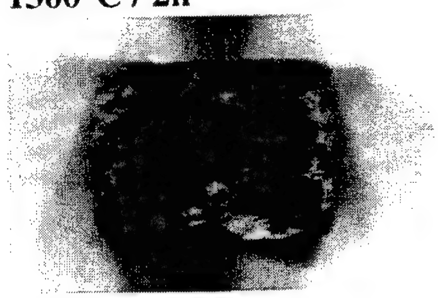

Mo-30V-22Si-8B
1300°C / 200h

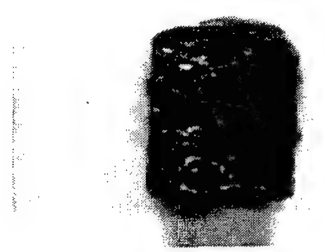

Mo-30V-15Si-8B
1300°C / 2h

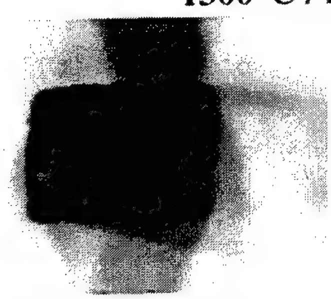

Mo-25V-22Si-6B
1300°C / 200h

Figure 15. Macrophotographs of Selected Mo-Si-B Alloys Exhibiting Shape Change at 1300 °C

For the lowest Si content (i.e., 12Si, metal phase + 3:1 silicide + T2 phases) both at 800 °C and 1300 °C, there was excessive weight loss, within a few cycles, as shown in Figure 16.

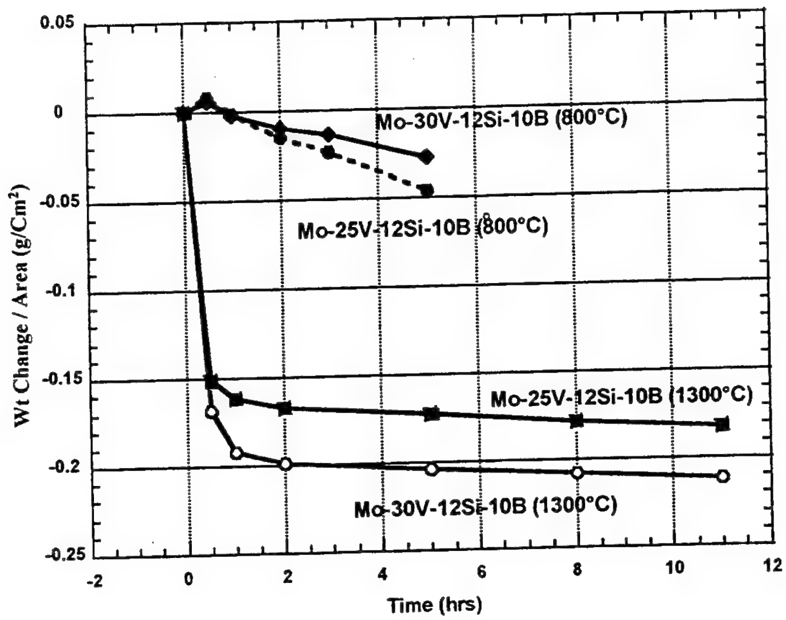

Figure 16. Cyclic Oxidation Kientics of Additional V-Containing Alloys (lower Si) at 800 °C and 1300 °C

Thus, in general, the V-containing alloys do not exhibit improvement in oxidation behavior over that for the base Mo-Si-B composition.

3.4 Mo-Re-Si-B Alloys

3.4.1 Phase Relations

The chemistries of various phases, as determined by EPMA, are given in Table 6.

Table 6. Phases as Determined by EPMA for Various Mo-Re-Si-B Alloys

Alloy: Mo-7.5Re-7.5Si-10B		
Element	**Metal Phase**	**T2**
Mo	82.1	62.7
Re	11.2	1.4
Si	3.2	12.4
B	3.5	23.5

Alloy: Mo-12Re-8Si-10B		
Element	**Metal Phase**	**T2**
Mo	69.3	58.7
Re	16.2	2.6
Si	3.1	12.2
B	11.4	26.5

Alloy: Mo-15Re-20Si			
Element	**σ (MoRe)**	**$(MoRe)_3Si$**	**$(MoRe)_5Si_3$**
Mo	58.1	72.2	60.1
Re	29.2	3.1	3.1
Si	12.7	24.7	36.8

Alloy: Mo-20Re-15Si-10B			
Element	**σ (MoRe)**	**T2**	**$(MoRe)_5Si_3$**
Mo	44.7	57.4	56.2
Re	32.5	5.3	3.8
Si	10.1	12.8	36.5
B	12.7	24.5	3.5

Alloy: Mo-20Re-13Si-10B			
Element	**σ (MoRe)**	**T2**	**$(MoRe)_5Si_3$**
Mo	56.5	59.3	59.1
Re	26.0	3.9	2.4
Si	12.4	13.2	37.3
B	5.1	23.6	1.2

Alloy: Mo-12Re-12Si-10B				
Element	**σ (MoRe)**	**T2**	**$(MoRe)_5Si_3$**	**MoB**
Mo	27.8	31.3	30.3	46.8
Re	32.5	8.8	5.7	1.84
Si	10.9	13.0	36.5	10.17
B	12.4	25.4	3.2	41.19

Heat Treatment: 1550 °C/100 hr +1400 °C/100 hr

At 8 at.%Si and 12 at.%Re levels, T2 and metal phase were found to exist for 10 at.%B. It is probable that at these Re and B levels, but with slightly higher Si content, a three-phase metal + 3:1 silicide:T2 field, exists. However, with increasing Si and Re contents, the intermetallic σ phase (MoRe) field is extended to produce an equilibrium between σ + $(MoRe)_3Si$ + $(MoRe_5)Si_3$ phases. Figure 17 shows possible phase equilibria based on the data given in Table 7.

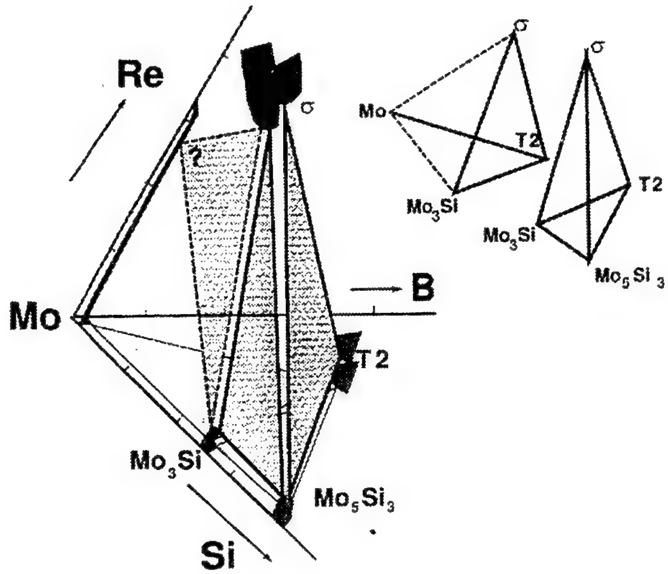

Figure 17. An 1400 °C Isotherm Construct for the Mo-Rich Corner of the Mo-Re-B-Si Phase Diagram Containing Two Four-Phase Fields Schematic

Table 7. Phases as Determined by EPMA for Various Mo-Re-Ti-Si-B & Mo-Re-Si-V-B Alloys

Alloy: Mo-20Ti-23Re-15Si-10B			
Element	**α (MoRe)**	**T2**	**$(MoRe)_5Si_3$**
Mo	27.8	31.3	30.3
Ti	16.4	21.54	24.3
Re	32.5	8.8	5.7
Si	10.9	13.0	36.5
B	12.4	25.4	3.2

Alloy: Mo-11Si-11B-5Al			
Element	**α (MoRe)**	**T2**	**$(MoRe)_5Si_3$**
Mo	28.4	32.1	36.1
Ti	18.3	23.3	18.4
Re	33.3	7.9	6.9
Si	13.6	12.3	37.6
B	6.4	24.4	1.0

Heat Treatment: 1500 °C/100 hr + 1400 °C/100 hr

The quaternary phase field construction also schematically includes the two four-phase fields, Mo + 3:0 T2 + σ and 3:1 + 5:3 + T2 + σ, respectively. Thus, the results indicate that, in this system, it is not possible to obtain a metal phase + 5:3 silicide + T2 equilibrium at 1700 °C, and such an equilibrium is not likely at other temperatures.

Two quinary alloys involving Ti and V, respectively, were also explored. There are indications from the literature that Ti and V additions suppress formation of the σ phase in the Mo-Re system. In the Mo-Ti-Re-Si-B and Mo-V-Re-Si-B compositions (Table 8) the results indicate σ + T2 + 5:3 silicide equilibrium in both systems at 1700 °C; therefore, the chosen levels of Ti and V, in the presence of other elements, did not eliminate the σ phase.

Table 8. Phase Chemistries as Determined by EPMA in Mo-Si-Ge, Mo-Si-Ge-B, and Mo-Si-B-Al Alloys

Alloy: Mo-11Si-5Ge		
Element	**Metal Phase**	**$Mo_3(SiGe)$**
Mo	95.9	77.1
Si	2.4	17.2
Ge	1.7	5.7

Alloy: Mo-11Si-5Ge-8B		
Element	**Metal Phase**	**$Mo_3(SiGe)$**
Mo	90.1	76.1
Si	2.3	16.3
Ge	1.6	7.6
B	6.0	-

Alloy: Mo-11Si-8Ge		
Element	**Metal Phase**	**$Mo_3(SiGe)$**
Mo	96.1	78.2
Si	2.1	12.8
Ge	1.8	9.0

Alloy: Mo-11Si-11B-5Al			
Element	**Metal Phase**	**$Mo_3(SiAl)$**	**T2**
Mo	93.4	71.5	59.1
Si	1.8	14.4	11.2
Al	3.9	8.6	0.4
B	0.9	5.5	29.3

Heat Treatment: 1600 °C/24 hr + 1700 °C/48 hr

3.4.2 Oxidation Behavior

Only limited oxidation experiments were carried out for a few compositions. The main results were, that while the 1300 °C oxidation response was comparable to that for the ternary Mo-Si-B alloy, at 800 °C the Re-containing alloys exhibited significant shape distortion due to swelling. Thus, the Re additions were not found beneficial for oxidation resistance.

3.5 Mo-Si-Ge, Mo-Si-Ge-B, and Mo-Si-B-Al Alloys

3.5.1 Phase Relations

The chosen alloy chemistries and the phases as determined by EPMA are given in Table 8. The ternary Mo-Si-Ge compositions were investigated to determine whether Ge can replace B and thus produce a Ge-SiO_2 protective glass during oxidation exposure. For these ternary compositions, as expected, the equilibrium phases were the metal phase and the Mo_3(SiGe). It was surprising that an addition of 8% B to the ternary Mo-Si-Ge did not produce the T2 phase. A higher level of B may be required to stabilize the three-phase metal + 3:1 silicide + T2 field. In the Mo-11Si-11B-5Al composition, the phases present were the metal phase, T2, and 3:1 silicide. Microstructural examination of the Al-containing alloy indicated that, for similar heat treatments, the phases were much finer than those in the ternary Mo-11Si-11B alloy.

3.5.2 Oxidation Behavior

At 1300 °C, all alloys exhibited weight losses significantly greater than that for Mo-11Si-11B for the equivalent number of cycles (by factors of 8 to 20 times). The shapes of the samples were reasonably intact, as shown by the macro photographs, Figure 18.

Mo-11Si-5Ge
1300°C / 6.5h

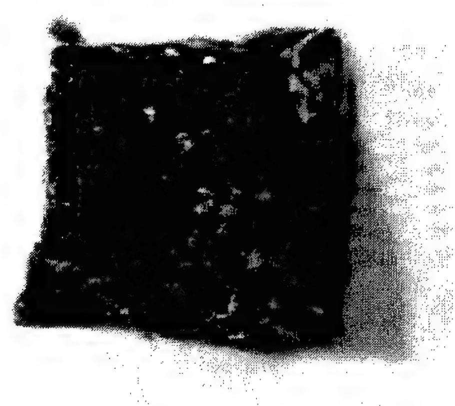

Mo-11Si-5Ge-8B
1300°C / 6.5h

Mo-llSi-8Ge
1300°C / 6.5h

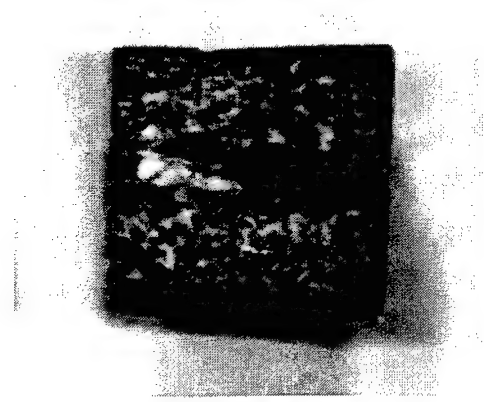

Mo-11Si-11B-5A1
1300°C / 6.5h

Figure 18. Macrophotographs of Ge- and A1-containing Mo-Si-B Alloys at 1300 °C

At 800 °C, Figure 19, however, the samples showed either complete delamination or incipient delamination after a few cycles.

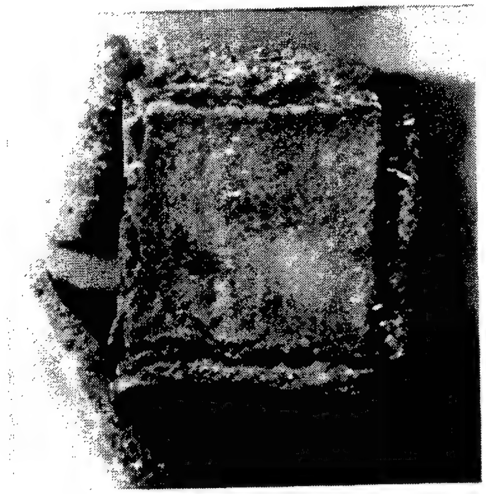

Mo-11Si-5Ge
800^{0}C / 1h

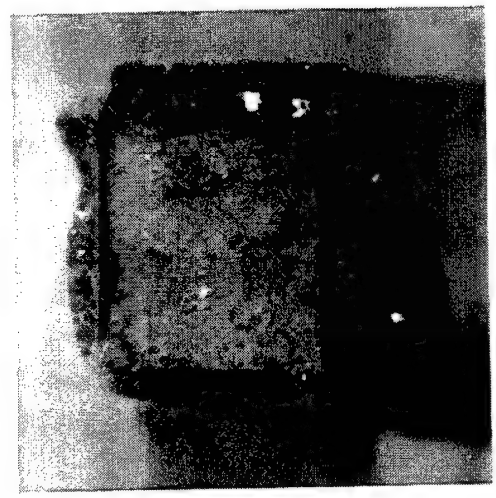

Mo-11Si-5Ge-8B
800^{0}C / 1h

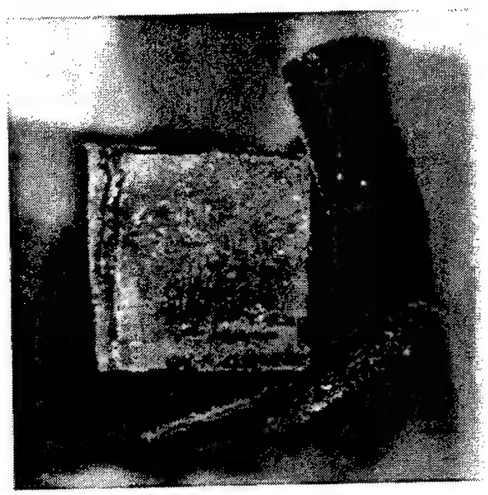

Mo-11Si-8Ge
800^{0}C / 1.5h

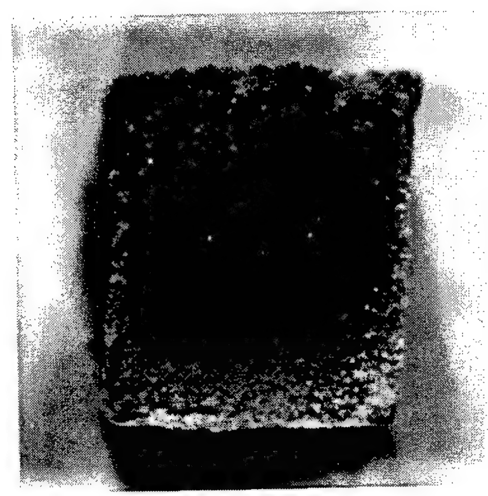

Mo-11Si-11B-5Al
800^{0}C / 1.5h

Figure 19. Microphotographs of Ge- and A1-Containing Alloys at 800 °C Showing Severe Delamination

Thus, at both temperatures, the oxidation resistance for the selected alloys was significantly inferior to that for the Mo-11Si-11B alloy.

3.6 Mo-Hf-Si-B and Mo-Ti-Cr-Si-B Alloys

Studies at Pratt & Whitney, under U. S. Air Force and Navy programs, [18], have shown that additions of small amounts of Hf to their ternary Mo-Si-B base alloys improve the oxidation resistance. Two different series of Hf-containing compositions were explored in the present work: 1) Mo-9Si-9B with Hf ranging from 0.5 to 10 at.%, and 2) Mo-12Si-12B with Hf from 0.3 to 3 at.%. In addition, an alloy with composition Mo-18Ti-11Cr-9Si-9B was also investigated; this composition is similar to that from Pratt & Whitney work. Ti and Cr were added to determine whether complex TiCr oxides form at the intermediate temperatures to provide some measure of oxidation protection. This part of the work was not performed to study the phase relations but mainly to carry out oxidation screening. The oxidation protection screening consisted of exposing the samples to static air at 800 °C and 1300 °C for 48 hours. The weight loss per unit area was compared to that for the baseline Mo-11Si-11B alloy. For the Hf-containing alloys, after the oxidation exposure, the shape change of the samples was recorded. For the Ti + Cr-containing alloys, cross-sectional microscopy of the oxide scale was carried out.

Figure 20 provides weight loss data for the Hf-containing compositions for 800 °C and 1300 °C exposures, respectively.

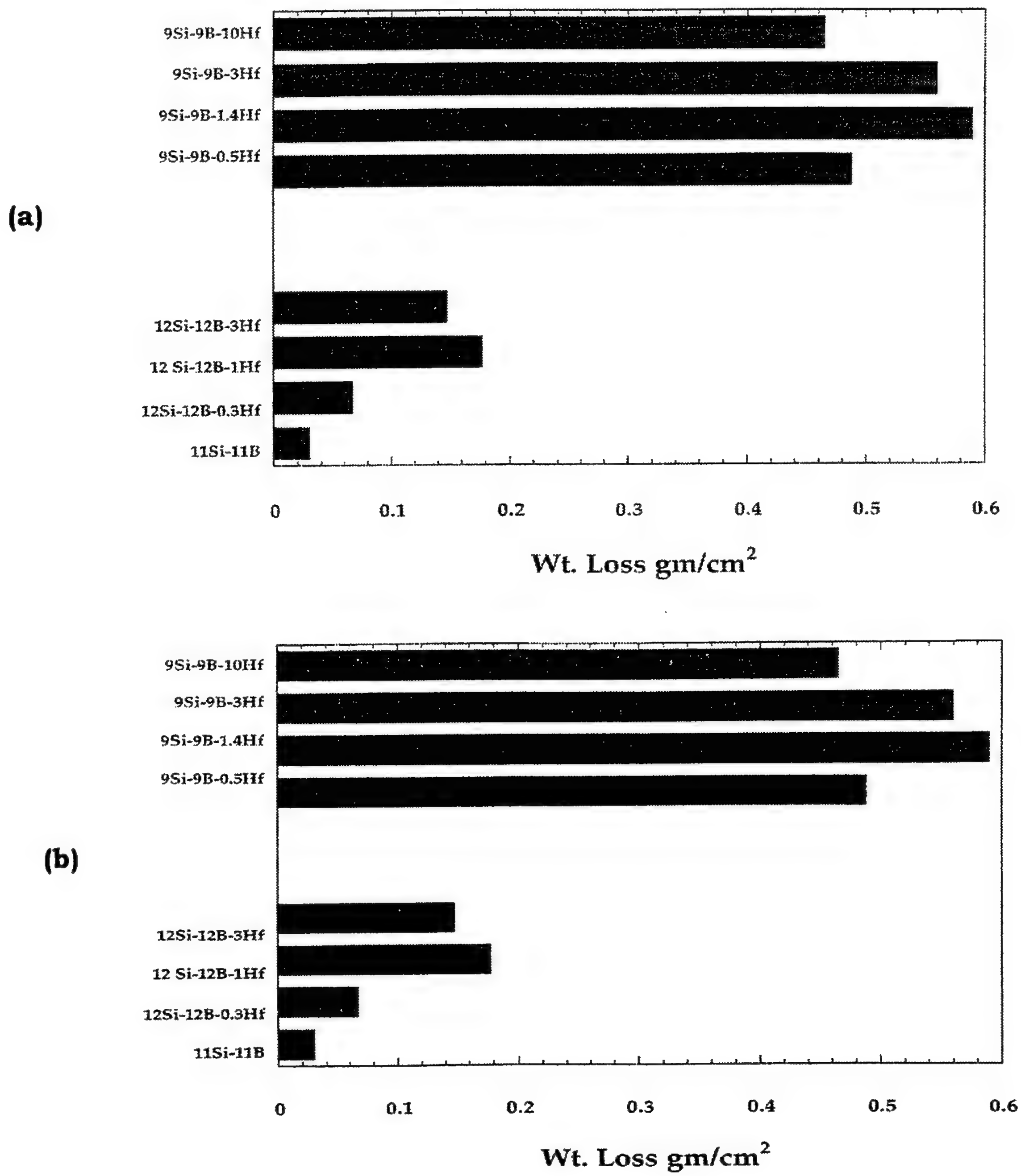

Figure 20. Weight loss /area for the Various Hf-Containing Mo-Si-B Alloys for 48 hr Oxidation Exposure (a) 800 °C, (b) 1300 °C.

At 800 °C all compositions except Mo-9Si-9B-0.5Hf exhibited weight losses higher than the base Mo-11Si-11B composition. The 9Si-9B-0.5Hf composition showed comparable weight loss. At 1300 °C, all Hf-containing compositions showed inferior oxidation resistance, based upon higher weight losses when compared to that for the base ternary composition. Figures 21 and 22 show the shape changes after oxidation exposures at the two temperatures.

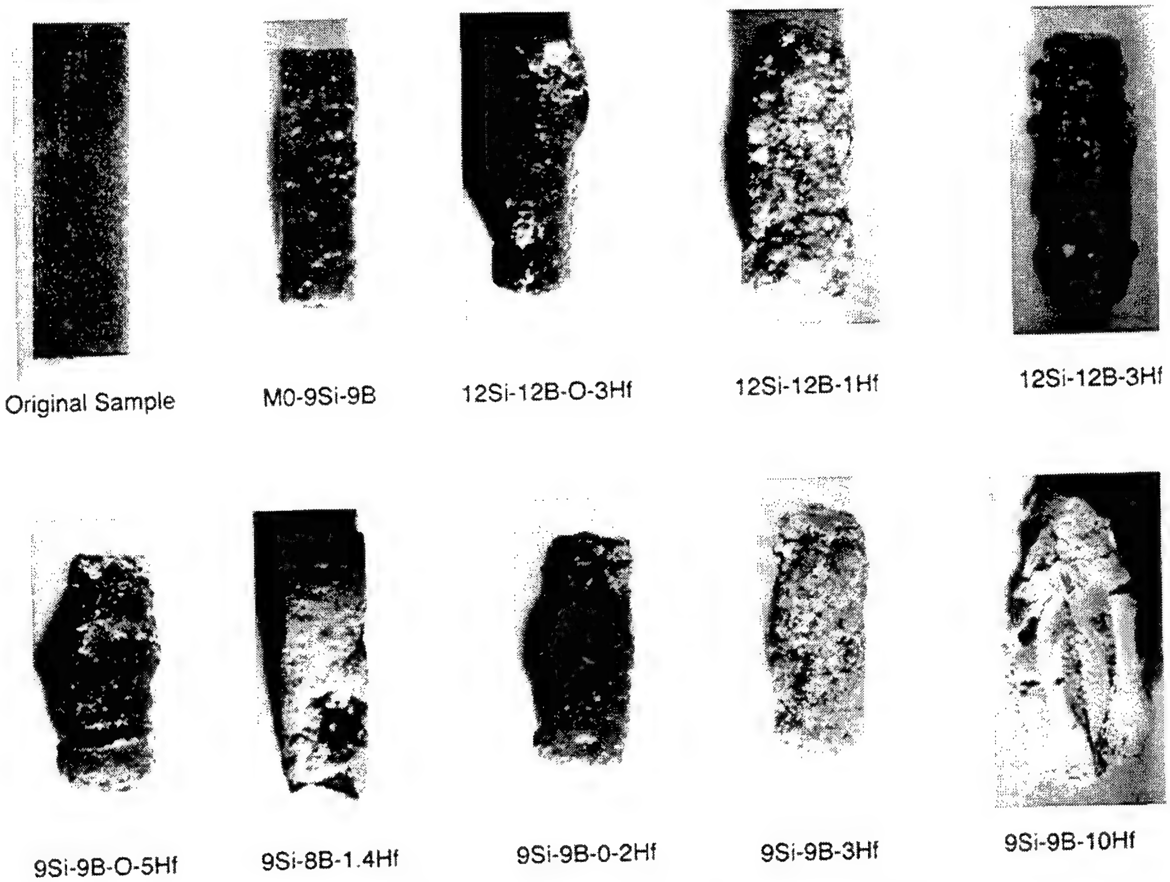

Figure 21. A Series of Microphotographs Exhibiting Changes in the Shape of Samples after 48-hr Oxidation Exposure: 800 °C

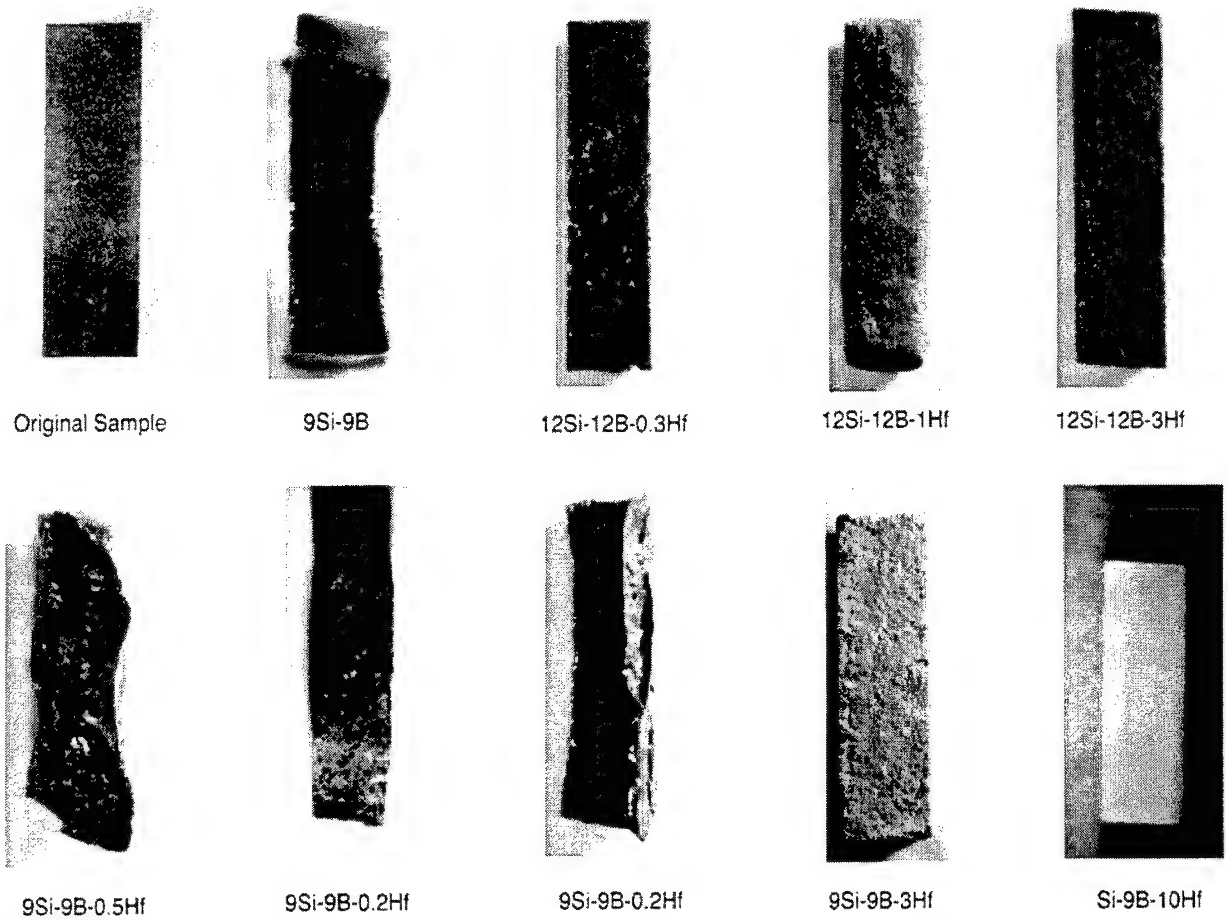

Figure 22. A Series of Microphotographs Exhibiting Changes in the Shape of Samples after 48-hr Oxidation Exposure: 1300 °C

At 800 °C, almost all compositions displayed significant shape change. At 1300 °C, the shape changes were minimal; however, in some cases, the B-SiO_2 glass appeared to have flowed excessively and dripped.

The weight losses, together with macro appearance of the samples, clearly indicated that Hf additions do not improve the oxidation resistance of the base Mo-Si-B composition.

Figure 23 shows the weight loss per unit area for the Mo-18Ti-11Cr-9Si-9B compared to the base Mo-Si-B ternary compositions at 800 °C and 1300 °C.

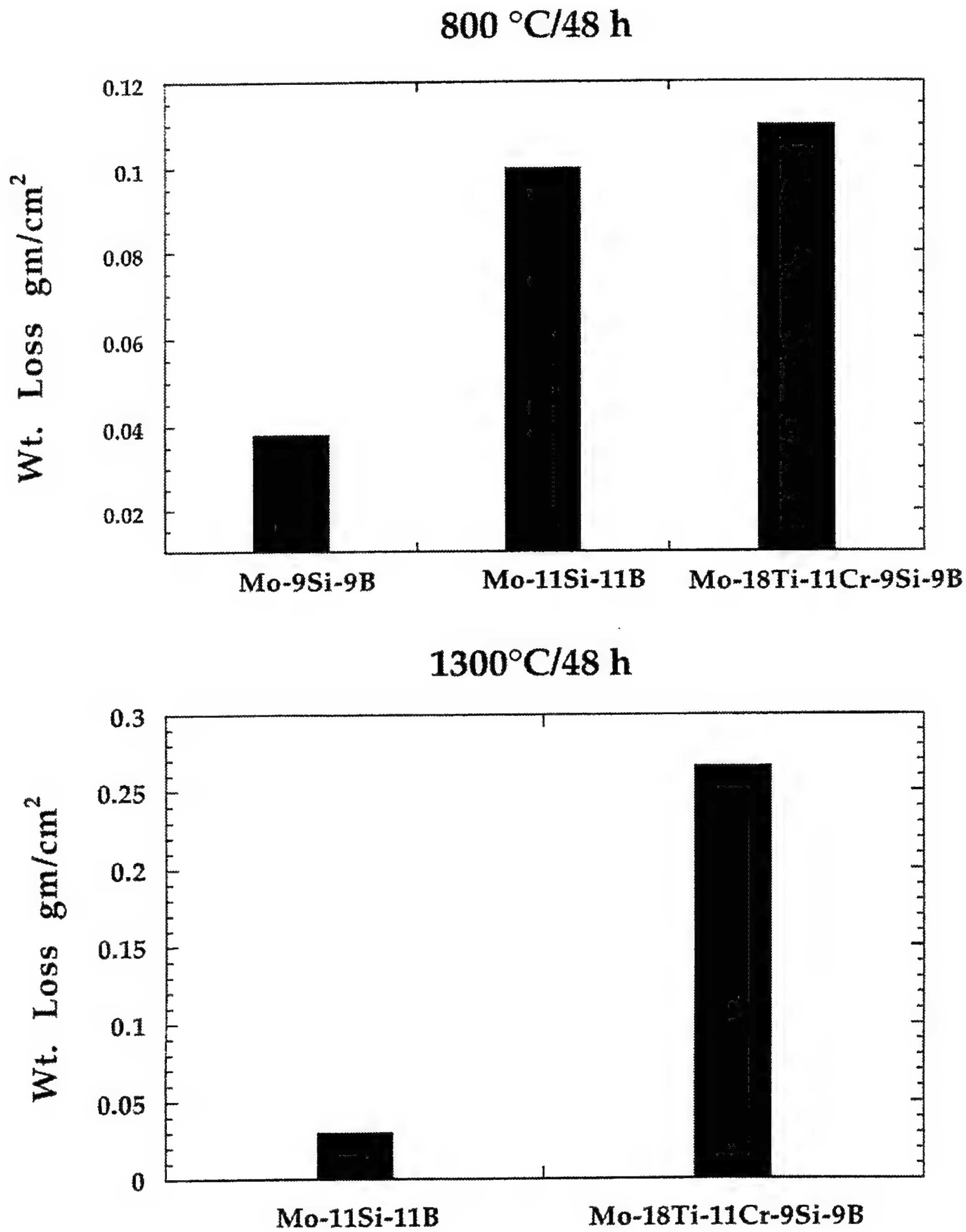

Figure 23. Weight Loss/Unit Area for the Ti+Cr-Containing Mo-Si-B Alloy as compared to the Base Ternary Composition for 48 hr Oxidation Exposure at: (a) 800 °C, (b) 1300 °C

The quinary alloy exhibited higher weight loss at both temperatures. Figures 24 and 25 show cross sections of oxide scales at the two temperatures.

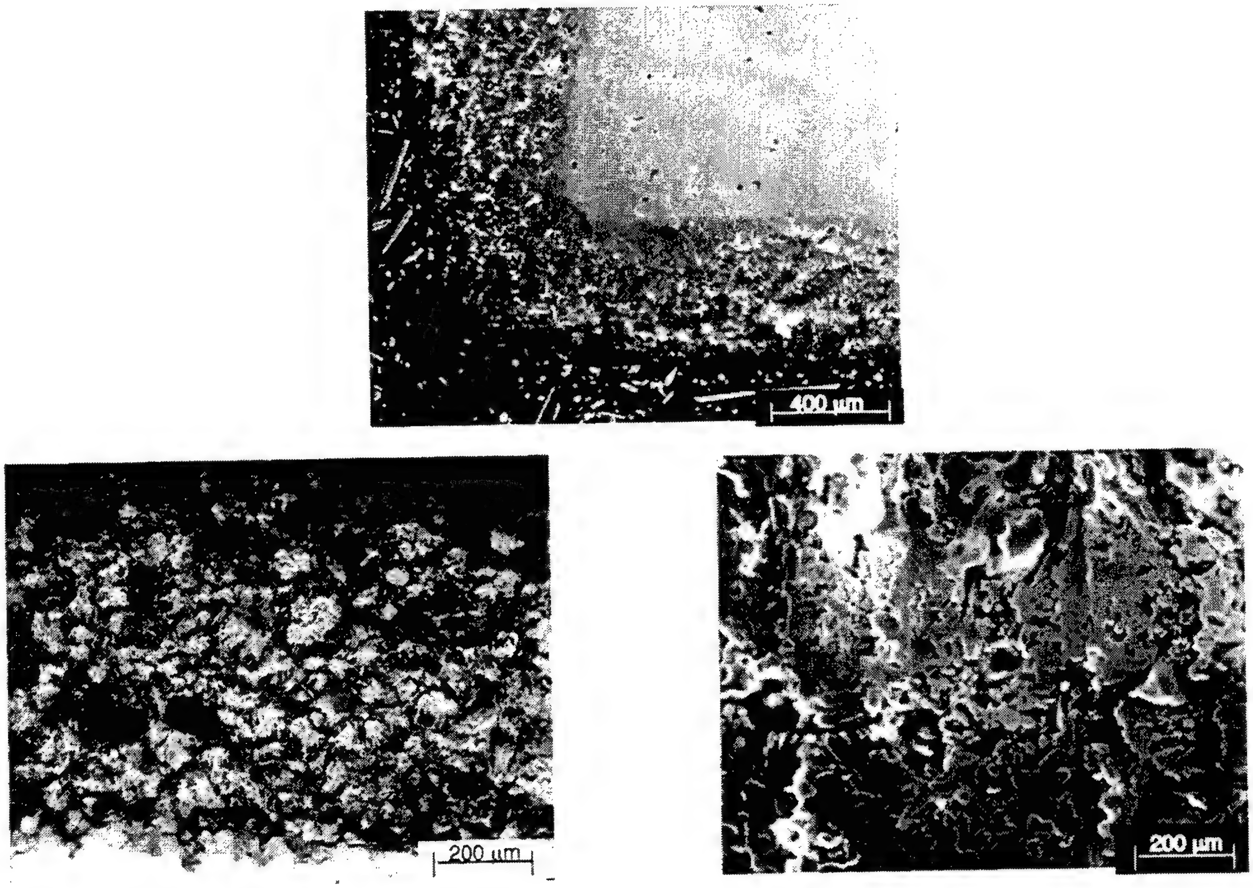

Figure 24. Cross Sectional SEM Micophotographs Showing Thick, Multiphased Oxide Scale for 48 hr Exposure at 800 °C

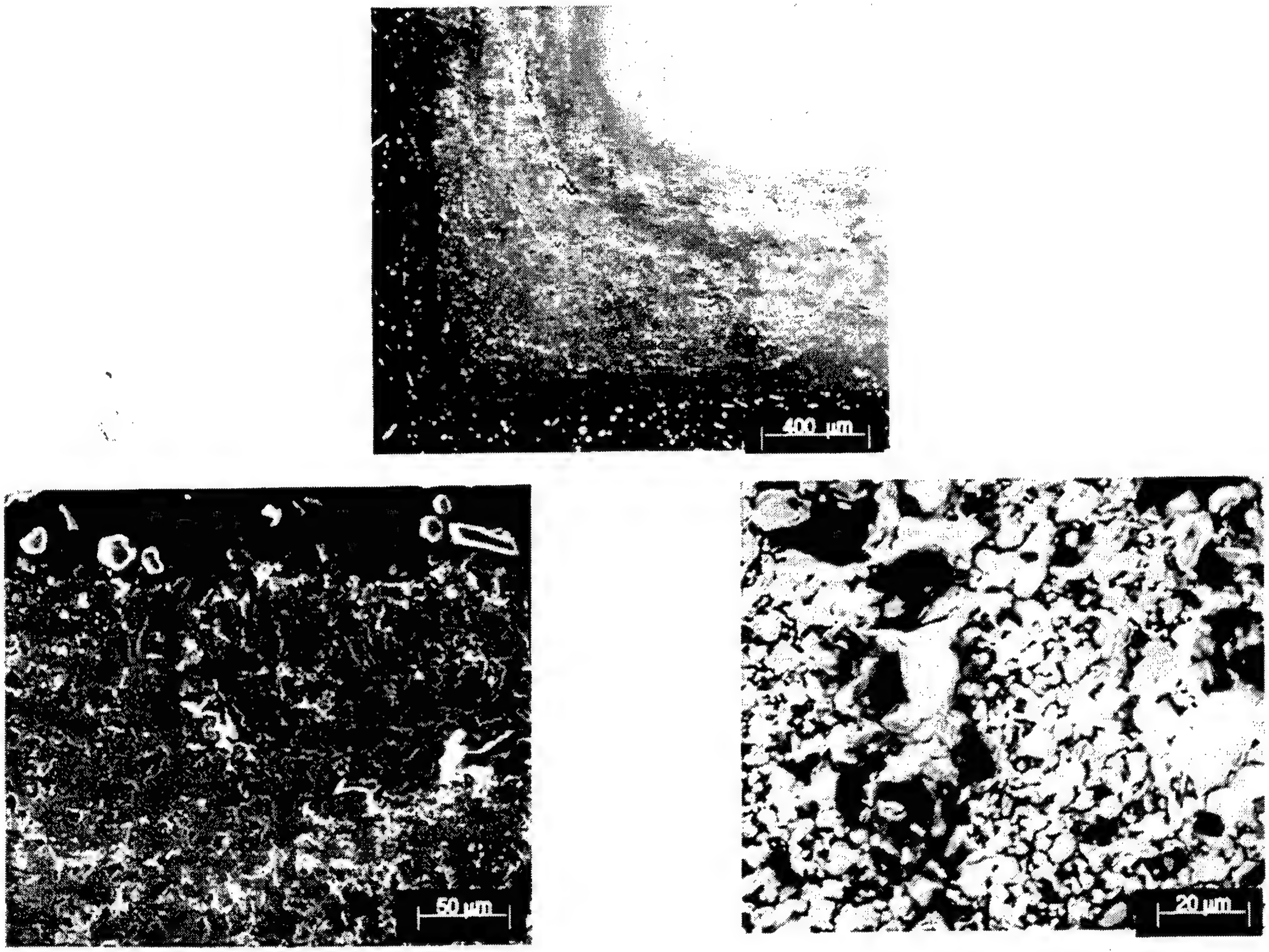

Figure 25. Cross Sectional SEM Micophotographs Showing Thick, Multiphased Oxide Scale for 48 hr Exposure at 1300 °C

Thick scales formed at both temperatures and the scales contained complex, multiphase oxides. No attempts were made to fully characterize these scales. The selected Ti + Cr additions to the base Mo-Si-B composition resulted in inferior oxidation resistance.

4. SUMMARY OF ALLOYING STUDY

The important findings of the effects of alloying additions to the base Mo-Si-B composition on phase relations and oxidation behavior are summarized below.

1. For W and Nb additions, it is possible to obtain a phase equilibrium consisting of the metal phase + 5:3 silicide + T2; however, this requires high levels of W (~ 30 at.%) and Nb (~ 25 at.%). The oxidation resistance for these high W- and Nb-containing compositions is inferior to the base Mo-11Si-11B, most probably due to selective oxidation of W and Nb, thus interfering with the formation of a continuous and protective B-SiO_2 glass.

For lower W contents, i.e., in the metal + 3:1 silicide + T2 phase field, the oxidation resistance is also inferior to the base ternary alloy at both 800 °C and 1300 °C. Lower Nb contents have not been investigated.

2. For Cr and V additions, the phase relations showed the existence of two three-phase fields: metal + 3:1 silicide + T2, and 3:1 silicide + T2 + 5:3 silicide. For no composition, it is possible to obtain metal + T2 + 5:3 silicide equilibrium. At 800 °C, all of the Cr- and V-containing alloys exhibited worse oxidation resistance than that for the base ternary. At 1300 °C the quaternary alloys exhibited oxidation resistance somewhat similar to that of the ternary alloys.

3. Re-additions produced complex phase relations and stabilized the intermetallic σ (MoRe) phase. Phase equilibria indicate the existence of a three-phase field, metal + 3:1 silicide + T2, and, two four-phase fields: metal + 3:1 silicide + T2 + σ, and 3:1 silicide + T2 + σ + 5:1 silicide. Limited oxidation experiments showed that Re additions were not beneficial for oxidation resistance.

4. Small amounts of Ge and Al additions did not alter the basic ternary Mo-Si-B phase equilibria. Oxidation resistance was found to be inferior in these compositions as compared to that in the ternary Mo-Si-B composition.

5. A number of Hf additions were explored at two different Si + B levels. At all levels, Hf additions did not improve the oxidation protections.

Thus, the most significant finding is that all alloying additions explored did not produce a better oxidation-resistant composition than the base ternary Mo-Si-B alloy. In fact, almost all alloying additions made the oxidation behavior significantly worse, leaving the ternary base alloy system with the best overall behavior achieved to date. It is possible that other alloying elements (e.g., rare-earth additions) might be worth exploring. However, it is not clear whether there is any scientific rationale for selection.

5. $MoSi_2$ BARRIER COATING ON Mo-Si-B ALLOYS

Since there is, at present, no obviously reasonable alloying approach for enhanced oxidation resistance beyond the behavior of the ternary base alloy, it was decided to explore application of a oxidation-resistant coating. A simple chemical vapor deposition (CVD) process was used to enrich the surface of a Mo-11Si-9B sample with Si. The base alloy was heat treated for homogenization at 1550 °C for 100 hours, followed by 1400 °C for 100 hours in argon. A coupon, ~ 5-mm cube, machined from the heat-treated alloy, was encapsulated in an evacuated quartz tube together with 1 g of Si powder and 20 mg of ammonium chloride and annealed at 850°C for 10 h. This process produced a uniform coating, ~ 25-μm thick, as shown in the BS SEM micrograph in Figure 26.

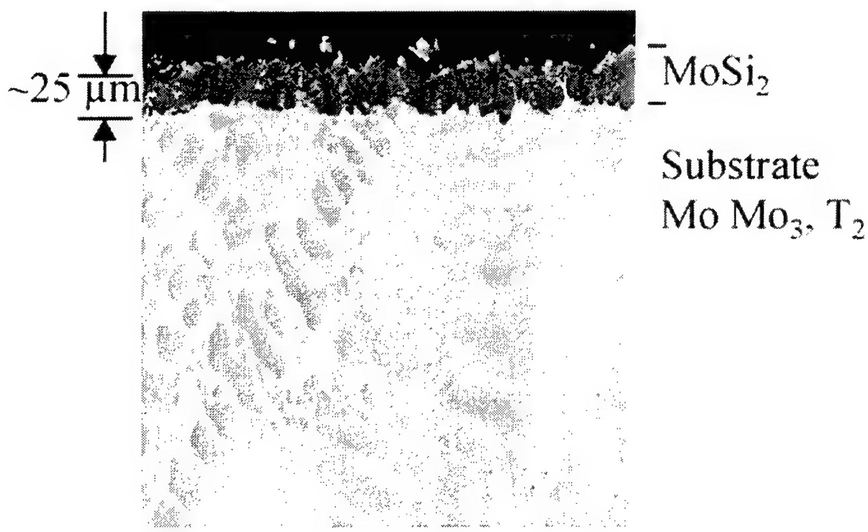

Figure 26. Microstructure of the As-Deposited MoSi2 Coating on Mo-10Si-13B Using a Simple CVD Process

Energy dispersive analysis (EDX) and X-ray diffraction revealed this coating to be $MoSi_2$. The coated coupon and an uncoated coupon were subjected to cyclic oxidation at 800 °C for 200 hours, followed by cyclic oxidation at 1300 °C for additional 200 hours. Figure 27 shows the weight loss data for both samples. The coated sample survived all of the cycles with virtually no loss of weight.

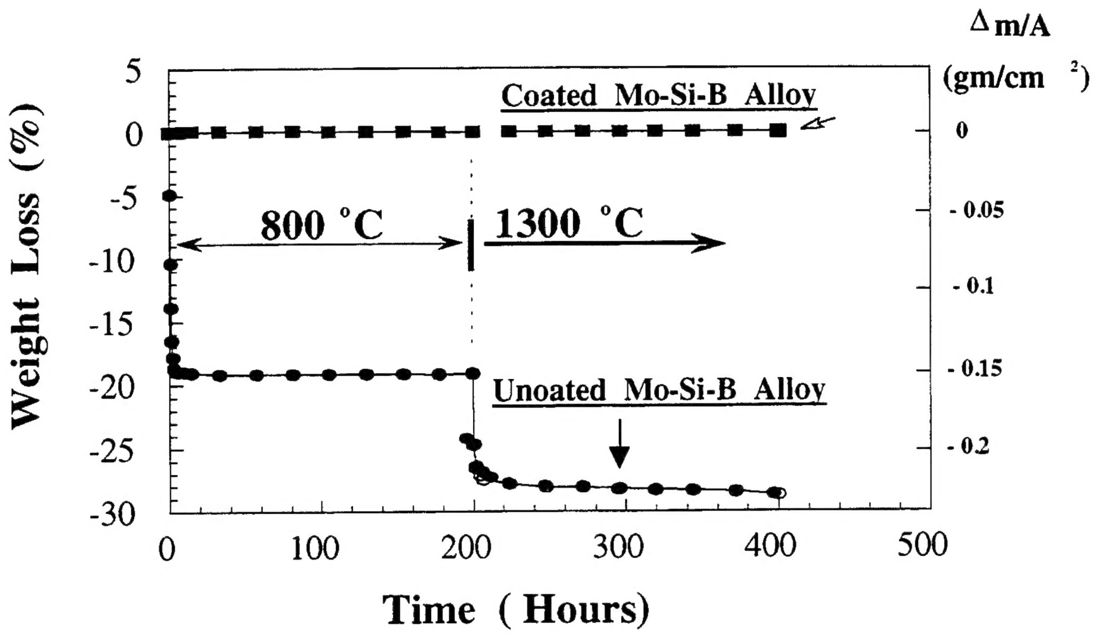

Figure 27. Comparison of the Oxidation Kinetics of the Coated and Uncoated Samples for Cyclic Exposure at 800 °C for 200 hr Followed by 1300 °C for 200 hr

In comparison, the uncoated sample exhibited considerable weight loss. Thus, a simple coating process (which has not been optimized) provides a high degree of protection.

As mentioned earlier, it is possible that the ongoing development efforts will not succeed in achieving adequate oxidation resistance in the Mo-Si-B-X alloys. Therefore, if a surface coating has to provide the only significant protection in service, then such a coating has to be the "prime reliant coating." This means that the coating must be highly reliable and durable, i.e., it should not fail under complex thermomechanical loading and environmental cycles present in a turbine engine. This necessitates further work on coating optimization and testing for reliability and durability. Such effort is presently underway.

6. CONCLUDING REMARKS

This study was undertaken to determine whether selected alloying additions to the base Mo-Si-B ternary composition can significantly enhance the oxidation resistance compared to Mo-11Si-11B. A number of alloying additions including W, Nb, Cr, V, Re, Ge, Al, Hf, and Ti + Cr did not enhance the oxidation resistance. In fact, in almost all cases the oxidation resistance became worse. Although not proven, this appears to be due to interference by the alloying elements to the formation of the protective B-SiO_2 scale.

A simple CVD coating process, which formed a $MoSi_2$ coating, provides oxidation protection both at 800 °C and 1300 °C. However, the coating has not been optimized and limits of its viability have not been determined. In addition, extensive work needs to be done to determine the reliability and durability of the coating.

7. REFERENCES

1. G. W. P. Rengstorff, *Trans. AIME,* 206,171 (1956).

2. M. Gleiser, W. L. Larsen, R. Speiser, and J. W. Spretnak, "Symposium on Basic Effects of Environment on Strength, Scaling, and Embrittlement of Metals at High Temperatures," *ASTM Special Technical Publication,* No.171, Philadelphia, PA, pp. 65-88 (1955).

3. J. J. Harwood, "The Metal Molybdenum", *American Society of Metals,* ed. J. J. Harwood, Cleveland, OH, pp. 420-461 (1958).

4. D. M. Berczik, "Methods for Enhancing the Oxidation Resistance of a Molybdenum Alloy and a Method of Making a Molybdenum Alloy," US Patent No. 5595616 (1997).

5. D. M. Berczik, "Oxidation Resistant Molybdenum Alloy", US Patent No. 5693156 (1997).

6. M.G. Mendiratta, T.A. Parthasarathy, and D.M. Dimiduk, AFRL/MLLM, Wright-Patterson AFB, OH, to be published.

7. T.A. Parthasarathy, M.G. Mendiratta, and D.M. Dimiduk, "Oxidation Mechanisms in Mo-Si-B Alloys," AFRL/MLLM, Wright-Patterson AFB, OH, *Acta Materialia,* in press.

8. C. A. Nunes, R. Sakidja, and J. H. Perepezko, in *Structural Intermetallics,* M. V. Nathal, et al., ed., TMS, Warrendale, PA, pp. 831-839 (1997).

9. C.A. Nunes, R. Sakidja, Z. Dong and J.H. Perepezko, *Intermetallics,* vol 8(4), pp. 327-337 (2000).

10. J.H. Schneibel, C. T. Liu, D. S. Easton, and C. A. Carmichael, *Materials Science and Engineering A,* vol 261, pp. 78-83 (1999).

11. J.H. Schneibel, M.J. Kramer, O. Unal and Richard N. Wright, *Intermetallics,* vol 9, pp. 25-31, (2001).

12. T.G. Nieh, J.G. Wang, and C.T. Liu, *Intermetallics,* vol 9, pp. 73-79, (2001).

13. R. Kiefler, O. Schob, H. Nowotny and F. Benesovsky, *Montash. Chem.,* vol 93, pp. 517-21, (1962).

14. E.M. Savitsky, V.V. Baron, M.I. Bychkova, S.A. Bakuta, and E.I. Gladyshevsky, Izv. Akad Nauk SSSAR, *Metall.,* pp.159-62, (1965).

15. Diagrammy Sostoianiia Metallicheskikh Sistem, N.V. Agee, ed., Viniti Press, Moscow, vol 10, pp. 182, (1964).

16. E.M. Savitsky, V.V. Baron, Yu. V. Efimou, and E.I. Gladyshevsky, Zh. Neorg. Khim, vol 7, pp. 1117-25, (1962).

17. T.B. Massalski, *ASM International*, Binary Alloy Phase Diagrams, ed., Materials Park, OH, (1990).

18. D. Berczik, Pratt & Whitney, East Hartford, CT, private communication.